

Vibrational Relaxation and Dynamical Transitions in Atactic Polystyrene

Paul Painter,^{*,†} Hanqing Zhao,[†] and Yung Park[‡]

Materials Science and Engineering Department, Penn State University, University Park, Pennsylvania 16802, and Department of Polymer Science and Engineering, Sunchon National University, 315 Maegokdong Sunchon, Jeonnam, Korea

Received August 21, 2008; Revised Manuscript Received December 2, 2008

ABSTRACT: Infrared bands and Raman lines recorded in the frequency domain have a counterpart in the time domain in the form of time-correlation functions, which are sensitive to molecular dynamics on the picosecond time scale. Time correlation functions and their variation with temperature have been calculated for the modes observed near 1601 and 1583 cm^{-1} in the infrared spectrum of atactic polystyrene. The correlation functions can be modeled by assuming that there is a fast relaxation process characterized by a single relaxation time that is inhomogeneously broadened by a slower process, also characterized by a single relaxation time. The fast modulation is of the order of 0.014 ps for both modes. Librational motions of the phenyl ring occur on the 0.01 ps time scale, suggesting that this mode of relaxation involves a rapid dephasing process. One cannot draw firm conclusions, however, because dephasing and vibrational energy relaxation mechanisms cannot be separated by studies of simple band shapes alone. A slower process, with a relaxation time of the order of 1–10 ps, inhomogeneously broadens both modes. The slower process for the 1601 cm^{-1} mode is relatively insensitive to temperature and mirrors the so-called “fast” transition seen in neutron diffraction studies of this polymer. The second fundamental mode, near 1583 cm^{-1} , is also inhomogeneously broadened, but the relaxation time calculated for this mode is far more sensitive to temperature as a result of anharmonic coupling to a combination mode that is probably mediated by lattice or bath modes. This provides a path for vibrational energy relaxation and sensitivity to dynamical transitions. A change in the modulation of the 1583 cm^{-1} band becomes apparent about 10–20 °C below the thermally measured T_g . Relaxation times at first increase (from about 2 ps to near 10 ps) then decreases and becomes negligible at temperatures near 180 °C. These results are consistent with theories of the glass transition, which predict a dynamical transition near $1.2T_g$ and a crossover region between this temperature and the laboratory T_g .

Introduction

The shapes and widths of infrared bands and Raman lines in the spectra of condensed matter are influenced by both static and dynamic effects—so-called inhomogeneous broadening together with dephasing processes and vibrational energy transfer.^{1–17} In the disordered state, there is a distribution of local environments, and as a result, there is no longer a single transition energy associated with a particular normal mode, but a band. Even if the distribution of frequencies is random about a mean, however, the resulting band is not necessarily Gaussian. Assuming the normal modes on each molecule in a system are excited simultaneously, because they have slightly different frequencies (as a result of interactions and small differences in local environments), they get out of phase with one another as time progresses, resulting in destructive interference. The shape and breadth of a band then depend on how fast this happens. If dephasing is fast, the effects of local differences in environment are averaged out by a rapid “loss of memory”, and this can result in what is termed “pure phase relaxation” and a Lorentzian profile.

Vibrational energy can relax by resonance transfer processes and by transfer to other, lower energy modes whose vibrations may be coupled to the mode of interest or to overtone or combination modes that are close in frequency. Low-frequency lattice or “bath” modes can play an important and intriguing role in this process. If, for example, a combination mode is separated from a fundamental by a few wavenumbers, a lattice or bath mode can “make up” the energy difference between the

fundamental and the overtone, ensuring a conservation of energy and providing a mode of relaxation.⁶ This could result in a sensitivity of the high-frequency-mode band shape to relaxation phenomena like the T_g . In previous work we have observed such a coupling of one of the ring modes of *a*-PS to a combination mode through a bath mode.^{18,19}

Unfortunately, infrared bands and Raman lines in ordinary or linear spectra are a convolution of various dynamic as well as static effects, and their contributions cannot be separated directly.²⁰ However, if a model is assumed, significant insight into the dynamics of the system can still be obtained. Here we will expand on our recent work on atactic polystyrene (*a*-PS) using a wider temperature range and a modified method of analysis, correcting what we now believe to be an erroneous assumption. This allows us to probe two phenomena of direct relevance to an understanding of the glass transition: fast processes that occur on the time scale of a few picoseconds and a dynamical crossover temperature that can be observed at temperatures of about $1.2T_g$.

The nature of the glass transition and the various relaxation processes that occur at both higher and lower temperatures is a subject that has a rich and deep literature, involving a wide range of theoretical approaches and experimental studies, as described in various reviews.^{21–25} In terms of interpreting the experimental results presented here, one model and two microscopic theories are important. Ngai’s coupling mode model^{26–28} predicts that there is a crossover time, t_c , of the order of 2 ps. At times shorter than this, relaxation has a simple initial exponential (Debye) form, but at longer times it follows a Kohlrausch–Williams–Watt (KWW) function. A so-called “fast process”, with relaxation times in the picoseconds range, observed in a number of

* To whom correspondence should be addressed.

[†] Penn State University.

[‡] Sunchon National University.

experimental studies (as reviewed in refs 21 and 22), has been identified with the short time regime ($t < t_c$) in Ngai's model.²⁹

The fast process has some of the characteristics of the β_{mc} relaxation of mode-coupling theory. (We append the subscript mc to differentiate this from the slower, secondary β transition.) Mode coupling theory (MCT) develops a picture of the dynamics of glass-forming liquids through a consideration of density fluctuations. It predicts that there is a critical temperature, T_c , where the diffusional motion characteristic of the liquid state becomes arrested as molecules or chain segments become trapped in a cage of their neighbors. (This is often described as an ergodic to nonergodic transition.) The β_{mc} relaxation is predicted to be strongly related to the α relaxation (glass transition) and a characteristic feature of all glass-forming materials.

MCT inspired many experiments and has been successful in a number of its predictions. However, studies of a wide range of materials demonstrated that the fast process begins to appear at temperatures well below T_g and is therefore not related to the β_{mc} relaxation, at least at low temperatures (see ref 21 and citations therein). Furthermore, the glass transition predicted by MCT at T_c is always higher than that determined experimentally, but if the original theory is modified to include thermally activated "hopping" processes, the arrest of structural relaxation at T_c is prevented.^{29–31}

Wolynes and co-workers have taken a different approach in their development of random first-order transition theory (RFOT).^{25,32–34} This approach uses free energy functionals to describe the stability of states of nonuniform density. One result that is directly relevant to the work reported here is the prediction of a temperature, T_A , at which a dynamical transition occurs, corresponding to the onset of activated motion in the liquid. Above this temperature, the time scales for molecular collisions and the interchange of positions are about the same, but as the liquid is cooled to T_A , molecules begin to reside within a cage of their neighbors and persistent local structures are formed. Interconversion between these structures continues below T_A but near the experimentally observed T_g become so slow that only a fraction of the rearrangements have time to occur. There is an obvious correspondence between T_A and T_c of MCT, and Kirkpatrick and Wolynes³⁵ have pointed out that the two theories are essentially equivalent at the dynamical crossover.

The rest of this paper will be organized as follows: First, we will describe the spectroscopic experiments and how we obtain band-shape parameters and correlation functions; we will then consider how relaxation times are obtained by fitting these correlation functions to a model; finally, we will discuss the results in the context of the models and theories mentioned above.

Experimental Section

The atactic polystyrene ($M_w = 190\,000$) used in this study was obtained from Scientific Polymer Products, Inc. Thin films were prepared by casting 4% (w/v) THF solutions onto KBr windows. The solvent was removed slowly under ambient conditions for a minimum of 24 h. The sample was then dried in a desiccator for an additional day. After that, the sample was placed in a vacuum oven at 120 °C to remove residual solvent. (Note that at lower temperatures not all of the THF is removed.)

Infrared spectra were obtained on a Digilab FTS-45 Fourier transform infrared (FTIR) spectrometer using a minimum of 256 co-added interferograms at a resolution of 1 cm^{-1} . All films were sufficiently thin to be within the absorbance range where the Beer–Lambert law is obeyed. A custom-made horizontal cell holder was used to prevent loss of sample due to flow at elevated temperatures. Films were heated in 10 °C stages to chosen

temperatures and held at these temperatures while spectra were recorded.

Spectroscopic Results

We previously reported a detailed description of our methodology and the spectroscopic changes that occur in the infrared spectrum of *a*-PS as a function of temperature in the range 30–150 °C.¹⁸ We will not repeat the discussion here but will emphasize one point previously made and make additional observations concerning the use of standard curve resolving programs.

One cannot overemphasize the importance of choosing a baseline correctly and reproducibly when analyzing band-shape changes. Most polymers have a large number of overlapping bands in the mid-infrared region of the spectrum, and the characteristics of these modes (shape, width at half-height, etc.) have to be determined by curve fitting. One usually chooses the region of the spectrum that is of interest and limits the analysis to this region. In many studies, baselines are then often defined so as to connect two points defining local minima in the spectra, on the assumption that there is no absorption at these frequencies (although scattering and other effects will result in the absorption values being nonzero). However, the intensity of a Lorentzian (Cauchy) peak is about 1% of the peak height at a distance of 10 times the width at half-height from the frequency of maximum absorption. In addition, as soon as one examines the infrared spectrum of a polymer in any detail, one usually finds weak overtone, combination modes, "hot bands", etc., which complicate matters considerably, so choosing a baseline is not trivial. Adding to the problems, many commercial software packages have automatic baseline correction routines. These usually adjust all or chosen minima in the spectrum to an assumed zero absorbance value. This can lead to significant distortions in band shape, particularly when applied to spectra with strongly curving baselines. In addition, the curve resolving or deconvolution packages included with most modern instruments often set the baseline to the absorbance values defined at the first and last wavenumber positions of the region defined by the user. This can lead to huge errors. There are other problems with these packages that we will return to below.

Our interest is in the 1600 cm^{-1} region of the spectrum of *a*-PS. We initially chose this region because defining a baseline was to some degree straightforward.¹⁸ In addition, there are two conformationally insensitive, fundamental normal modes of vibration in this wavenumber range, near 1601 and 1583 cm^{-1} , respectively, at room temperature. They are both in-plane, "ring-breathing" modes.^{36,37}

In order to set the baseline and curve-resolve the bands in this wavenumber range, a much broader region of the spectrum was initially examined. Figure 1 shows the infrared spectrum of atactic polystyrene obtained at 28 °C. The baseline appears to be linear but has a slight slope. The inset in this figure shows the region between 2200 and 450 cm^{-1} . By narrowing the absorbance scale to between 0.05 and 0.1 absorbance units, we observed that between 2200 and 1100 cm^{-1} (where the background transmission is at a maximum) the baseline appears to be linear, to a very good approximation. We did not initially set the baseline to the absorbance values defined by minima near these points, however. Because the wings of Lorentzian bands extend a long way from their center (affecting the minimum near 1100 cm^{-1} , identified by an arrow on the plot) and because of the presence of weak overtone/combination bands (affecting a minimum near 2050 cm^{-1} , also identified by an arrow on the plot), we initially set the baseline to 0.002 absorbance units below these points. This choice is somewhat arbitrary and based on 1% of the maximum absorption of the 1600 cm^{-1} band (about 0.2 units for the films we prepared).

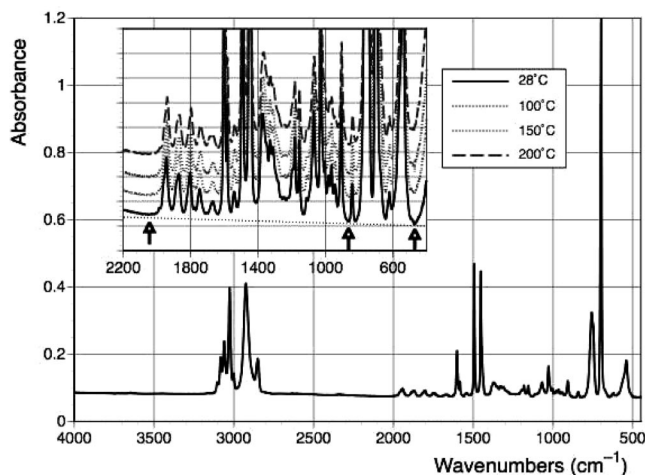


Figure 1. Infrared spectrum of atactic polystyrene. The inset shows spectra taken at different temperatures and the points used to define the position of a linear but sloping baseline.

Curve resolving was also performed for baselines set at the minima and at values of 0.001 units below the minima. We then looked for slight deviations between calculated and experimental spectra. Baselines set at 0.001 units below the minima appeared to be best on a visual basis. Our experience is that least-squares criteria are not necessarily a good measure of fit, in that bands that make no spectroscopic sense but give an excellent fit can often be produced by the unwary. A clear warning sign is that bands that are unusually broad (sometimes 100 cm^{-1} or more in width at half-height) are generated, as curve-fitting programs try to compensate for poorly chosen baselines or the presence of unaccounted for modes. (Of course, certain bands, such as the OH stretching mode in hydrogen-bonded systems, can be that broad, but this is obvious to the naked eye and such factors do not apply to *a*-PS.)

As the temperature is increased, the absorbance value of each of the minima in the spectra increases systematically, so that the baseline has to be defined separately for each spectrum. In addition, at the higher temperatures used in this study ($>150^\circ\text{C}$), the baseline shows a pronounced upturn at low wavenumbers relative to baseline absorbance values at higher wavenumbers, as indicated by the arrow near 500 cm^{-1} placed on the inset in Figure 1. The baseline still appears to be linear in the limited region of the spectrum of interest here, however, and we continued to use minima near 1100 and 2050 cm^{-1} to define the baseline.

The results of curve-resolving the 1600 cm^{-1} region of the spectra of *a*-PS obtained at 40 and 140 $^\circ\text{C}$ are shown in Figure 2. The spectra were curve-resolved using a program developed in our laboratories. Experimental bandwidths are often a convolution of Gaussian and Lorentzian (Cauchy) shapes (resulting in a Voigt profile), but these are often approximated using a sum function. We use the following expression:

$$I(\nu) = fA_0 \exp[-\ln 2[(\nu - \nu_0)/\Delta\nu_{1/2}]^2] + (1 - f)A_0 / \{1 + [(\nu - \nu_0)/\Delta\nu_{1/2}]^2\} \quad (1)$$

The Gaussian and Lorentzian shapes that combine to make up the overall band profile are assumed to have equal half-widths at half-height, $\Delta\nu_{1/2}$, and are present in the proportions of f to $(1 - f)$. A_0 is the peak height, ν_0 is the wavenumber coordinate of the peak maximum, and ν are the frequencies of the points that describe the bands. Liu et al.³⁸ have shown that this particular sum function is actually an excellent approximation to a true Voigt profile.

On the basis of criteria discussed previously,¹⁸ the 1600 cm^{-1} region of the spectrum was fit to six bands. Examining Figure 2, it is apparent that both the 1575 and 1592 cm^{-1} modes are very weak at low temperatures, and one might question their presence. But they display a significant increase in intensity as the temperature is raised and are clearly evident to the naked eye in spectra obtained at high temperatures ($T > 100^\circ\text{C}$).¹⁸ Initial estimates of the half-width, peak height, and band shape (fraction Gaussian) were input to the program, and before least-squares fitting the summed profile was compared to the experimental spectrum. Parameters were adjusted to obtain a reasonably close correspondence. (The fit can diverge if one starts out with too big a difference.) Different starting points for parameters such as the band shape were tried, particularly for spectra obtained at temperatures above 80 $^\circ\text{C}$. For spectra obtained at lower temperatures, the parameters quickly refined to consistent values. As the temperature of the sample approached the T_g , a large number of iterations were required to obtain convergence, however. The number of iterations required depended on the initial parameters. We found that curve-resolving sequentially, with parameters obtained for a spectrum obtained at say 80 $^\circ\text{C}$ being used as a starting point for the spectrum obtained at 85 $^\circ\text{C}$, gave good results. Curve-resolving was performed in this fashion as a function of both ascending and descending temperature, and the results were averaged. Values of the parameters then converged quickly to consistent values at low and high temperatures, but for spectra obtained over a temperature range of about 80–140 $^\circ\text{C}$ a larger number of iterations were still required and more scatter in the data was encountered, as discussed later.

We also tested a number of commercial curve-resolving programs in an attempt to fit to a true Voigt profile, which some claimed to allow. Either these did not work at all (the program gave no results, only regurgitated initial parameters) or when they did would only refine around the starting values of the parameters. In other words, if you initially defined a band to be Gaussian, that is the final band shape that you would get. For the same band, an initial starting definition of a Lorentzian profile would ensure that this was your final answer. The programs were obviously constrained to refine around initial chosen values, presumably to speed the process. Users need to run a number of checks on these programs using bands of initially defined shape in order to determine their utility in studies such as that reported here.

We previously reported changes in the frequencies and absorption (band areas) of the fundamental modes near 1601 and 1583 cm^{-1} as a function of temperature.¹⁸ Plots of these parameters showed a change in slope near T_g . The maximum temperature reached in this previous study was 150 $^\circ\text{C}$, but in work reported many years ago that covered a wider temperature range, Enns et al.³⁹ observed similar changes and also a transition at higher temperatures that was then labeled the T_{II} transition. We obtained similar results, so here we will focus on changes in bandwidths and band shapes. However, a plot of that ratio of the band areas of the fundamental near 1583 cm^{-1} to that of the area of the combination mode near 1592 cm^{-1} is shown in Figure 3, illustrating the increase in intensity of the latter as the temperature is increased. Note also that there is an apparent change in behavior near temperatures of 90, 120, and 160–170 $^\circ\text{C}$.

Plots of the bandwidths (full width at half-height, $2\Delta\nu_{1/2}$) of the modes near 1601 and 1583 cm^{-1} are plotted as a function of temperature in Figure 4. The width of the 1601 cm^{-1} band increases with temperature in an apparently linear fashion in the temperature range 25 $^\circ\text{C}$ to about 90 $^\circ\text{C}$ and also in the range 140–200 $^\circ\text{C}$, but the points in a transition zone between 100 and 140 $^\circ\text{C}$ appear to be slightly above the trend lines. The

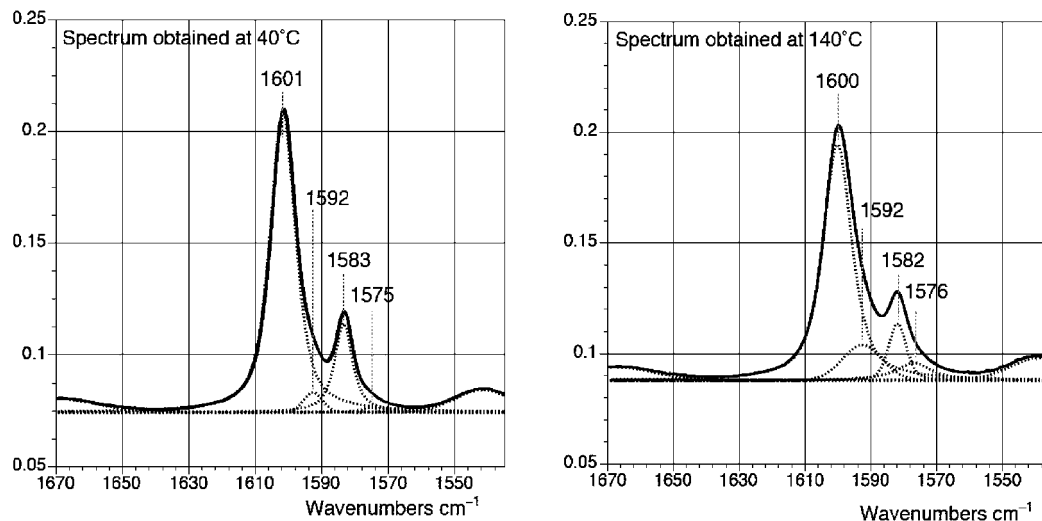


Figure 2. Results of curve-resolving the 1600 cm^{-1} region of the infrared spectrum of atactic polystyrene held at temperatures of $40\text{ }^{\circ}\text{C}$ (left) and $140\text{ }^{\circ}\text{C}$ (right). The profile of the original spectra and those obtained by adding the curve-resolved bands coincide.

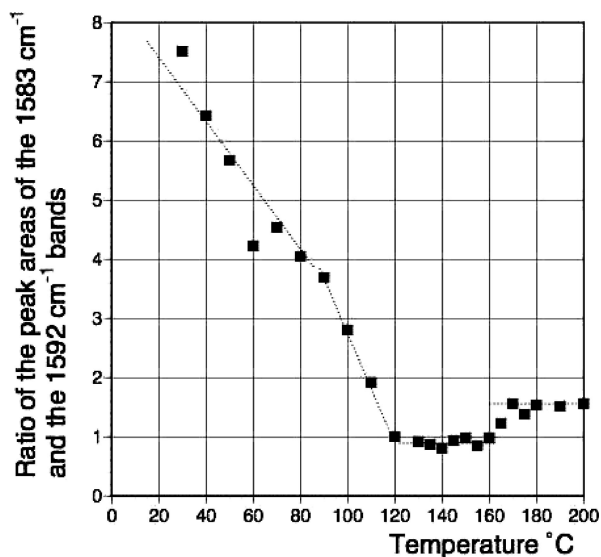


Figure 3. Ratio of the band areas of the 1583 cm^{-1} and 1592 cm^{-1} modes plotted as a function of temperature. The lines have been placed only as a guide to the eye.

differences are small and are probably within the error of the measurements, however. The width of the 1583 cm^{-1} band shows far more dramatic changes. For this latter mode, a transition zone between temperatures of about 100 and $140\text{ }^{\circ}\text{C}$ is clearly observed. Similar observations apply to the band shape, plotted in Figure 5 as the fraction Gaussian (f in eq 1). These parameters are subject to much greater error (changes in f of ± 0.05 do not make much difference in the fit). Accordingly, we cannot draw any conclusions concerning changes in the shape of the 1601 cm^{-1} mode. It apparently becomes less Gaussian as the temperature increases, but the changes are too small to reveal any sensitivity to transitions. The 1583 cm^{-1} mode shows significant changes, however. The bars in the figure show the range of values determined for studies on two samples: one curve-resolved twice (ascending and descending temperature), with the baseline set 0.001 absorbance units below the minima near 2050 and 1100 cm^{-1} and also with the baseline set 0.002 absorbance units below these minima. The range of values is small at low temperatures (below $80\text{ }^{\circ}\text{C}$, with an anomaly at $60\text{ }^{\circ}\text{C}$ that was reproducible in two experiments using different films) and also at high temperatures ($>180\text{ }^{\circ}\text{C}$), where the band was determined to be purely Lorentzian in all

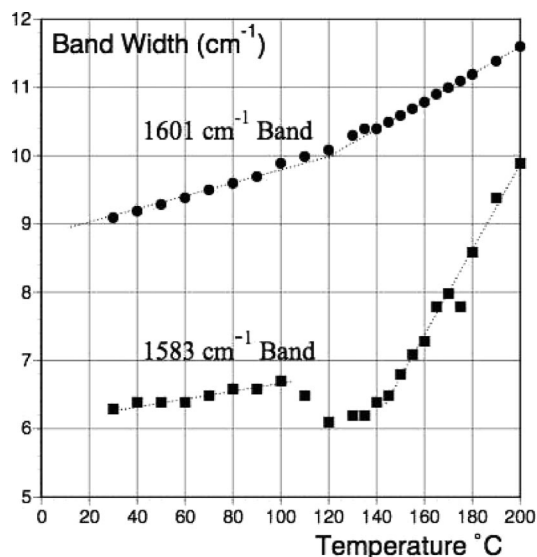


Figure 4. Plot of the bandwidths of the 1601 and 1583 cm^{-1} bands as a function of temperature. The lines have been placed only as a guide to the eye and are not the result of a fitting process.

experiments. It can be seen that even within the errors inherent in setting the baseline and curve-fitting, there is a clear change in band shape. At temperatures greater than about $80\text{ }^{\circ}\text{C}$, the band becomes increasingly Gaussian, reaching a maximum in the range 130 – $140\text{ }^{\circ}\text{C}$, but as the temperature increases beyond $140\text{ }^{\circ}\text{C}$, this tendency is quickly reversed and the shape of the band becomes essentially Lorentzian at temperatures greater than about $180\text{ }^{\circ}\text{C}$.

The 1583 cm^{-1} band is more sensitive to temperature than the mode near 1601 cm^{-1} , apparently as a result of coupling to low-frequency modes through a Fermi resonance interaction with a close-lying combination mode.¹⁸ Although both fundamentals are within 10 cm^{-1} of the combination mode near 1592 cm^{-1} , the 1583 cm^{-1} band has A_1 (local) symmetry and can therefore engage in Fermi resonance interactions with the combination mode near 1592 cm^{-1} , which also has A_1 symmetry. The 1602 cm^{-1} mode has B_1 symmetry and cannot engage in a similar interaction.

It appears that the coupling of the 1583 and 1592 cm^{-1} modes through lattice or bath vibrations becomes more pronounced as the latter become thermally excited. In this regard, a calculation

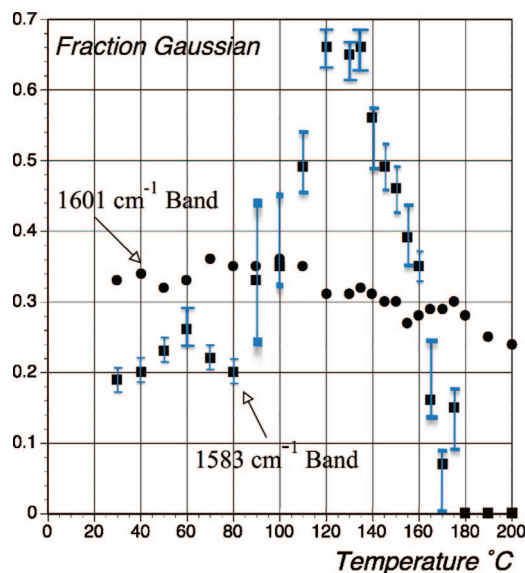


Figure 5. Band shape of the 1601 and 1583 cm^{-1} modes, expressed as a “fraction Gaussian” (f in eq 1), plotted as a function of temperature.

of time correlation functions associated with these bands provides considerable insight, in spite of the well-known limitations of this type of analysis.

Calculation of Time Correlation Functions

In order to calculate time correlation functions from spectroscopic data, various difficulties must be overcome. First, any band-shape distortions introduced by the instrument must be taken into account. The FTIR data used in this study had a ratio of apodized resolution to full width at half-height of between 0.11 and 0.16, so band-shape corrections were considered unnecessary. Second, a baseline must be correctly identified and set. We discussed the identification of the baseline at length above and believe it can be established with only small errors, as long as careful attention to sample preparation is paid.¹⁸ Third, in using infrared spectroscopy, the variation of the refractive index across an absorption band must be taken into account. However, for the relatively weak modes that are the subject of this study, it has been found that the refractive index varies between values of about 1.47 and 1.49 across the band profile,⁴⁰ so corrections for this factor were neglected. Finally and most crucially, a way must be found to deal with the overlap of modes commonly found in polymer materials.

In this study, we used the curve-resolving methodology described above. An experimental band profile is simply a series of data points, so if a function gives an exact fit to this profile (or one that is within the precision of the data), it seems reasonable to assume that the time correlation function calculated by numerical Fourier transformation of this band is a close representation of the original data. Accordingly, we generated bands using the parameters obtained from curve-resolving: the intensity at maximum absorption (A_0), the full width at half-height ($2\Delta\nu_{1/2}$), and the band-shape parameter (fraction Gaussian, f), using eq 1. The frequency of each band maximum, ν_0 , was set to 0 cm^{-1} . Band absorbance values were normalized to unit band area (to partially account for local fields⁷). The bands were generated out to $\pm 150 \text{ cm}^{-1}$, and the resolution of the original FTIR data was 1 cm^{-1} . Upon numerically Fourier transforming the bands (using a program written in MATLAB), this gave a frequency correlation function that, in principle, is reliable to 16 ps at a time resolution of about 0.17 ps.¹ Calculated correlation data were normalized to a value of 1 at $t = 0$.

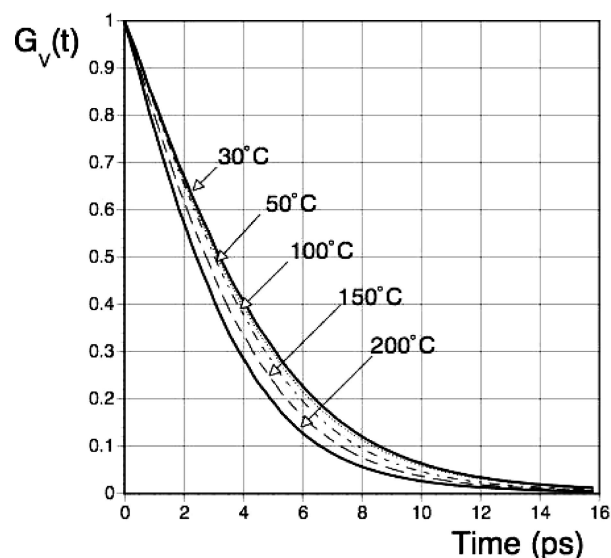


Figure 6. Plot of time correlation functions calculated for the 1601 cm^{-1} band of *a*-PS at selected temperatures.

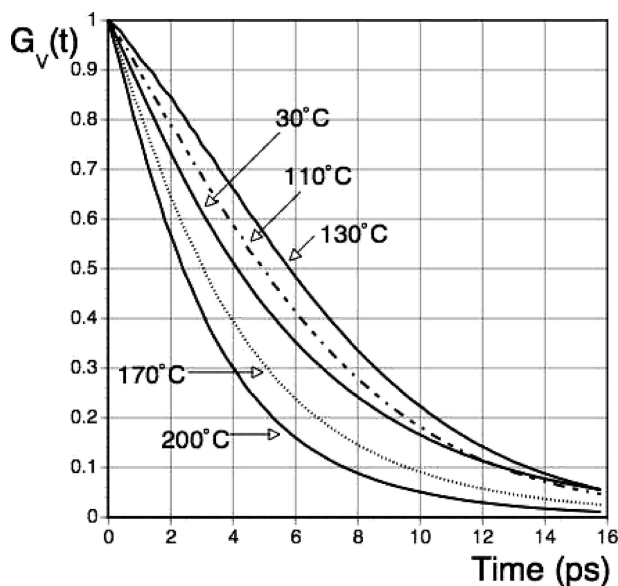


Figure 7. Plot of time correlation functions calculated for the 1583 cm^{-1} band of *a*-PS at selected temperatures.

The time correlation functions ($G_V(t)$) calculated for the 1601 and 1583 cm^{-1} bands are shown in Figures 6 and 7, respectively. For the 1601 cm^{-1} band, there are relatively small changes in $G_V(t)$ as the temperature is increased from 25 to 200 °C, with faster correlation decay at higher temperature, reflecting a small broadening of the band. Essentially, the trends seen in our previous study,¹⁹ which terminated at 150 °C, continue up to 200 °C. In contrast, $G_V(t)$ calculated for the band near 1583 cm^{-1} changes significantly at temperatures in the 140–150 °C range. As before,¹⁹ the correlation decay becomes slower as the temperature is increased to about 140 °C (in contrast to the faster decay of the 1601 cm^{-1} mode), reflecting the change in band shape of this mode, which becomes more Gaussian as the temperature is increased (see Figure 5). This trend is entirely reversed at higher temperatures, however, and the decay in correlation time then increases significantly up to temperatures of 200 °C. In order to gain further insight into these changes, we calculated relaxation times using a modified model due to Kubo.⁴¹

The Kubo Model and Inhomogeneous Broadening

The stochastic line-shape model of Kubo,⁴¹ adapted to vibrational spectroscopy by Rothschild,⁵ has been a crucial tool in analyzing line and band shapes.¹⁻¹⁷ The model assumes that local variations in environment, hence interactions, are random about a mean, so that the distribution of modes takes a Gaussian form. The variance of the fluctuations is equal to the second moment of a band contour, M_2 , given by

$$M_2 = \frac{\int_{-\infty}^{+\infty} I_{\text{vib}}(\omega)(\omega - \omega_0)^2 d\omega}{\int_{-\infty}^{+\infty} I_{\text{vib}}(\omega) d\omega} \quad (2)$$

It is assumed that each of the individual modes that contributes to a profile is characterized by a correlation function that decays exponentially with a correlation time τ_c , $\exp(-t/\tau_c)$. Using these assumptions, the following expression for the vibrational time correlation function is obtained:⁴¹

$$G_V(t) = \exp\{-M_2\tau_c^2[\exp(-t/\tau_c) - 1 + t/\tau_c]\} \quad (3)$$

There are two limiting regimes defined in terms of $M_2^{0.5}\tau_c$: at very short times ($t \rightarrow 0$) or, in what is called the slow modulation limit (modulation frequency $\sim 1/\tau_c$), $M_2^{0.5}\tau_c \gg 1$:

$$G_V(t) = \exp(-0.5M_2t^2) \quad (4)$$

Because the time correlation function is Gaussian, its Fourier transform results in a Gaussian band shape, one that reflects the distribution of local environments.

At very long times ($t \rightarrow \infty$) or in the fast modulation limit, $M_2^{0.5}\tau_c \ll 1$, the time scale of the fluctuations, τ_c , in the system is small (hence the modulation frequency fast) and the time correlation function is exponential.

$$G_V(t) = \exp(-t/\tau_r) \quad (5)$$

where

$$\tau_r = \frac{1}{M_2\tau_c} \quad (6)$$

The Fourier transform of this exponential gives a Lorentzian band shape. The corresponding time correlation function is then a simple exponential, and the characteristic time, τ_c , is given by the reciprocal of the half-bandwidth at half-height $\Delta\omega_{1/2}$:

$$\tau_c = (\Delta\omega_{1/2})^{-1} = (2\pi c\Delta\nu_{1/2})^{-1} \quad (7)$$

In this equation ν is in wavenumbers (cm^{-1}) and c is the velocity of light.

In the slow modulation limit, the line shape is described as being inhomogeneously broadened. We will refer to this limit as static inhomogeneous broadening because the term inhomogeneous broadening is also used to describe the effect of a second, slower modulation superimposed upon a fast modulation (more on this shortly). In the fast modulation limit, the line shape is described as being homogeneously broadened and is characterized by an ensemble average homogeneous dephasing time that has contributions from both vibrational energy relaxation and pure dephasing. Accordingly, even in the fast modulation limit, an analysis of the resulting Lorentzian lines or bands cannot (without other information) provide a measure of pure dephasing, a goal of many studies of liquids, because it provides detailed insight into the fast dynamics (sub-picoseconds) of the system. Our focus is not on dephasing, however,

but on a spectroscopically slower process, on the picoseconds time scale. Confusingly, in terms of relaxation studies mentioned in the Introduction, this process is referred to as fast.

Although many of the band and line shapes of liquids appear to be largely Lorentzian, George, Auweter, and Harris⁴² showed a number of years ago that there is also what is termed inhomogeneous broadening in simple non-hydrogen-bonded liquids. One at first might consider that the Kubo model (or a corresponding model developed by Kirillov¹⁷) could readily interpolate between the limits of Gaussian and Lorentzian profiles, but the model is constrained by the experimentally determined second moment of the profile and cannot fit data where relaxations occur on more than one time scale. However, various studies have found that in a number of systems experimental data could be modeled in terms of two processes: a fast modulation and a second slower modulation that inhomogeneously broadens the band. The latter is a separate phenomenon from static inhomogeneous broadening, which reflects the distribution of environments encountered at very short times ($t \rightarrow 0$). George et al.⁴² found a correlation between the slow process and local density fluctuations and developed a theory that describes the line shape as a convolution of these two effects. The frequency correlation function can then be written as a product of two correlation functions:

$$G_V(t) = \Phi_h(t)\Phi_i(t) \quad (8)$$

As George et al.⁴² and Oxtoby⁴³ pointed out, this separation is only strictly valid if the homogeneous and inhomogeneous correlation functions decay on very different time scales. It is usual to assume that the correlation function of the modulation is exponential, so that both $\Phi_h(t)$ and $\Phi_i(t)$ can be written in the same form as eq 3. The homogeneous (rapid modulation) function is then

$$\Phi_h(t) = \exp\{-M_h\tau_h^2[\exp(-t/\tau_h) - 1 + t/\tau_h]\} \quad (9)$$

M_h is the contribution to the second moment of the band that is due to static inhomogeneous broadening (i.e., reflects the distribution of local environments at the moment the normal mode is excited). Inhomogeneously broadening is described by a second function of the same form:

$$\Phi_i(t) = \exp\{-M_i\tau_i^2[\exp(-t/\tau_i) - 1 + t/\tau_i]\} \quad (10)$$

The experimentally determined second moment of the band or line is then given by

$$M_2 = M_h + M_i \quad (11)$$

In our previous study,¹⁹ we assumed that the correlation function describing inhomogeneous broadening, $\Phi_i(t)$, was a simple Gaussian function, equivalent to allowing the relaxation time in eq 10 to be very long ($\tau_i \rightarrow \infty$). As a result, any changes in relaxation times could only be accommodated by changes in τ_h , which were calculated to be in the 0.01–0.02 ps range. Such changes may not be an accurate reflection of the underlying dynamics of the system if inhomogeneous broadening occurs on the picoseconds time scale. Indeed, studies of the “fast” process in polymers indicate that there is a relaxation on the time scale of about 1–10 ps,²¹ suggesting that a two-time-scale model would be more appropriate. Various theoretical models also predict a separation into two processes. For example, in the theory of Schweitzer and Chandler⁴⁴ short-range repulsive forces gives rise to a fast relaxation, while long-range attractive forces give rise to a slow modulation. As mentioned in the Introduction, Ngai’s coupling mode model^{26–28} also predicts that there is a so-called “fast process”, where a relaxation in

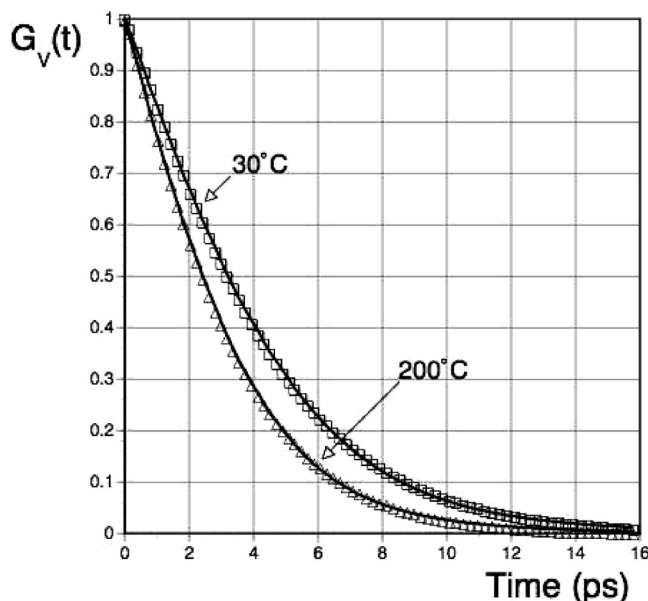


Figure 8. Fit of the correlation functions calculated for the 1601 cm^{-1} band of *a*-PS to a Kubo-type model that includes inhomogeneous broadening.

the picoseconds range has a simple initial exponential (Debye) form. Schmidt et al.⁴⁵ have analyzed this type of two-time-scale Kubo model and demonstrated that in certain limits it is capable of describing combined homogeneous and inhomogeneous broadening, even when the separation of the time scales is as low as a factor of 6. In the work we will report here, we will show that a two-time-scale model gives an excellent fit to the data and the difference in the time scales is of the order of 100. We believe that our previous assumption, that $\Phi_i(t)$ is a simple Gaussian function (i.e., $\tau_i \rightarrow \infty$), results in calculated values of the temperature dependence of the relaxation time, τ_h , that are unjustified.

Fits to the Model: Results and Discussion

It was demonstrated in our previous work that the original Kubo model (eq 3) could not fit the time correlation functions calculated for the 1601 and 1583 cm^{-1} bands, with the deviation between the model and the correlation functions calculated from experimental data increasing with increasing temperature.¹⁹ In the work reported here, we fit the data obtained from experiment using the assumption that relaxation is dominated by two processes, eqs 8–10, under the constraint imposed by eq 11, that the contributions of homogeneous and inhomogeneous broadening, M_h and M_i , to the band profile must sum to give the experimental second moment, M_2 . An excellent fit to the data was obtained. Figure 8 shows the fit obtained for the correlation function calculated for the 1601 cm^{-1} band, using the data for the highest and lowest temperatures as an illustration. Figure 9 shows equivalent fits for the correlation function calculated for the 1583 cm^{-1} band, comparing data obtained at 30 °C to that obtained at 110 and 130 °C, in the temperature range where the largest and most interesting changes are seen in the band shape.

Values of the relaxation times, τ_h and τ_i , and the second moments, M_h and M_i , are plotted as a function of temperature in Figures 10–13. It can be seen from Figure 10 that the fast modulation process (in vibrational spectroscopic terms) that we have associated with homogeneous broadening occurs in the sub-picosecond regime, with τ_h having values of the order of 0.014 ps for both modes at 25 °C. There is little change, if any, with temperature. The data for the 1601 cm^{-1} band shows far

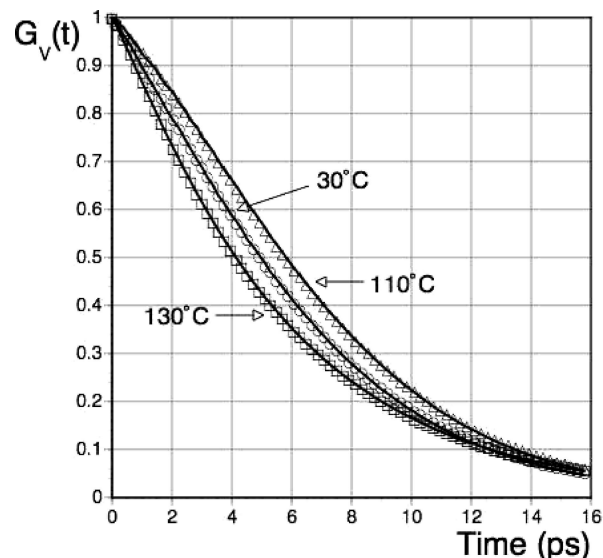


Figure 9. Fit of the correlation functions calculated for the 1583 cm^{-1} band of *a*-PS to a Kubo-type model that includes inhomogeneous broadening.

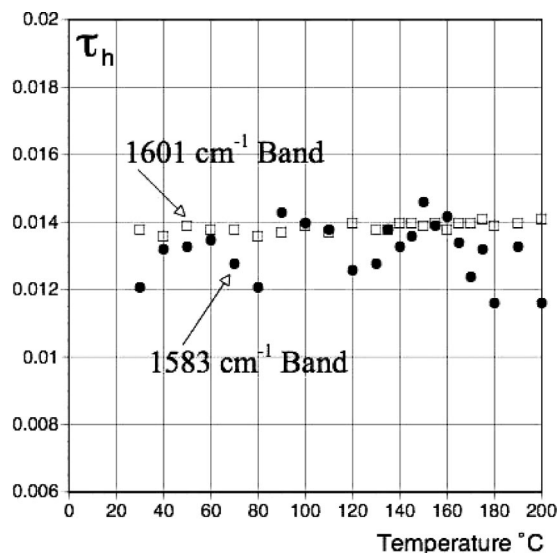


Figure 10. Plot of the correlation time, τ_h , calculated for the 1601 and 1583 cm^{-1} bands of *a*-PS as a function of temperature.

less scatter than those for the 1583 cm^{-1} band. This is because the former is more intense, and it is curve-resolved with greater accuracy and less error.

Although the contributions of vibrational energy relaxation and pure dephasing to the relaxation mechanism cannot be unambiguously separated, the data are consistent with a fast dephasing process. Tiller⁴⁶ calculated the dipole autocorrelation function of polystyrene in order to identify the characteristic motions that are important in dielectric relaxation. In addition to the motions occurring at frequencies below 120 cm^{-1} , which was the main concern of the study, large-scale motions associated with librations of the phenyl ring were observed in the range 500–700 cm^{-1} , corresponding to relaxations of the order of 0.01 ps. This fast modulation would be expected to lead to dephasing and also be relatively insensitive to transitions such as the T_g , where relaxations occur on far longer time scales. Essentially, motion of a phenyl ring in a local cage of neighbors would continue for many cycles before the cage relaxed. One would also expect that such a very fast homogeneous dephasing process would reflect the distribution of local environments that

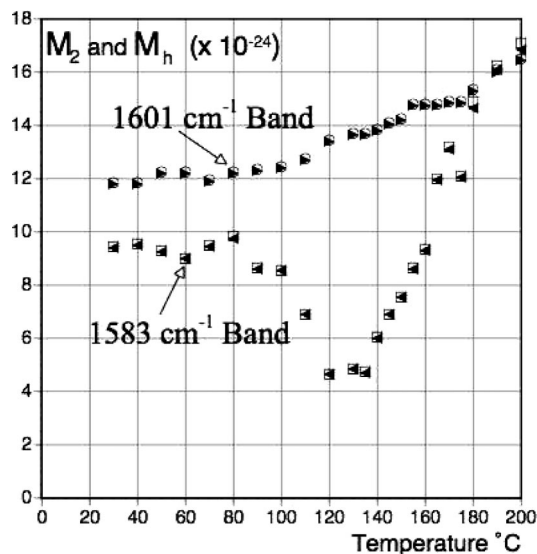


Figure 11. Plot of the contribution of homogeneous broadening and the second moment of the band profile for the 1601 and 1583 cm^{-1} bands of *a*-PS as a function of temperature: open data points, second moment; filled data points, contribution of homogeneous broadening to the second moment.

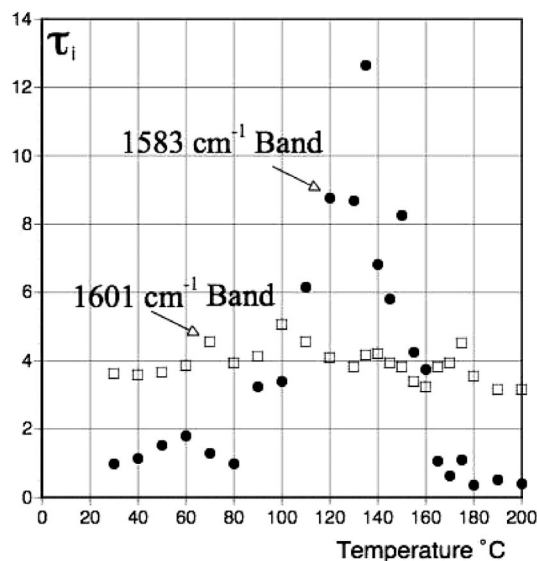


Figure 12. Plot of the correlation time characteristic of inhomogeneous broadening, τ_i , calculated for the 1601 and 1583 cm^{-1} bands of *a*-PS as a function of temperature.

would be encountered if other relaxations occurred on much longer time scales. The calculated values of M_h are compared to M_2 in Figure 11, and it can be seen that they almost superimpose, indicating that this fast relaxation provides the major contribution to the observed second moment (i.e., reflects static inhomogeneous broadening, the distribution of local environments as $t \rightarrow 0$).

For the 1601 cm^{-1} band, there is some sensitivity of both M_h and M_2 to temperature, with changes in the slope of the plots near the T_g and possibly near 180 $^{\circ}\text{C}$. However, the precision of the data is not good enough to make anything of this latter observation. In contrast, the second moment of the 1583 cm^{-1} mode changes dramatically at temperatures near 80 $^{\circ}\text{C}$, decreasing as the band shape becomes more Gaussian. Above temperatures of about 140 $^{\circ}\text{C}$, the trend is reversed, with the second moment increasing significantly as the band shape becomes more Lorentzian. (A true Lorentzian band has an infinite second moment and the tails of the band never return

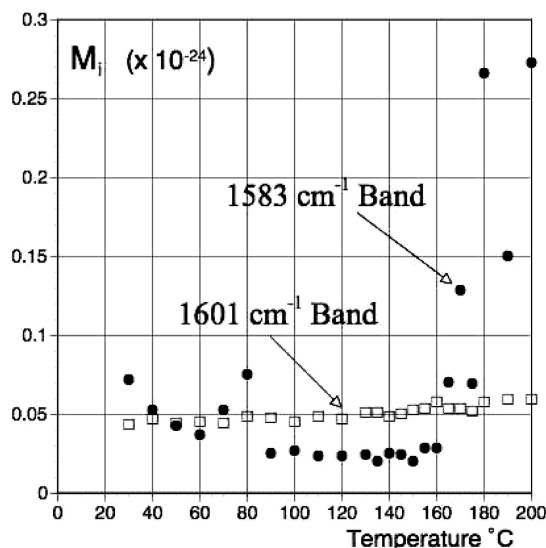


Figure 13. Plot of the contribution of inhomogeneous broadening to the second moment of the band profile for the 1601 and 1583 cm^{-1} bands of *a*-PS as a function of temperature.

to the “true” baseline, but within the errors of curve-resolving we cannot tell if we have a Lorentzian or almost Lorentzian band shape.)

The variation of the relaxation times associated with inhomogeneous broadening with temperature, τ_i , is shown in Figure 12. For the 1601 cm^{-1} band, essentially no change with temperature is seen, with a relaxation time associated with inhomogeneous broadening that is of the order of 4 ps. Dephasing processes that occur on this time scale would be expected to be sensitive to the “fast process” in the picoseconds range observed in neutron scattering studies,²¹ identified with the short time regime in Ngai’s model.²⁹ This “fast” relaxation is relatively insensitive to temperature,²¹ suggesting that dephasing on this time scale is contributing to inhomogeneous broadening of the 1601 cm^{-1} band. If so, this would be a very interesting result and would also justify the use of a single exponential to describe the effect of inhomogeneous broadening. However, a high-frequency vibrational mode can also relax by transferring energy to a combination of lower frequency internal and (eventually) lattice or bath modes through anharmonic coupling.⁴⁷ This ability to descend a “ladder of vibrational energy” could be an important vibrational relaxation mechanism in polymers such as *a*-PS, with its large number of internal vibrations. The rate at which this occurs would depend on the proximity (in terms of frequency or energy) to other modes and their ability to couple, which for molecules like *a*-PS would be affected by factors such as the local (C_{2v}) symmetry of the ring. Vibrational energy relaxation would lead to a random modulation of the high-frequency mode and hence some degree of inhomogeneous broadening. To reiterate, “linear” spectroscopic experiments such as those reported here cannot distinguish between vibrational energy relaxation and dephasing but are clearly useful in identifying modes where studies using nonlinear spectroscopic tools would be fruitful.

This ability to descend a “ladder of vibrational energy” would appear to play a far more prominent role in the vibrational relaxation of the 1583 cm^{-1} band, with its proximity to a close-lying combination mode that has the correct symmetry for Fermi resonance interactions. It can be seen from Figure 12 that the relaxation time associated with inhomogeneous broadening is roughly constant ($\tau_i \sim 1\text{--}2$ ps) at temperatures up to about 80 $^{\circ}\text{C}$ and then increases to values of the order of 8–12 ps in the temperature range of about 120–150 $^{\circ}\text{C}$ (we cannot be more precise than this because of the errors involved in curve-

resolving the 1583 cm^{-1} band), before decreasing to very small values at temperatures above $170\text{--}180\text{ }^{\circ}\text{C}$. The band shape becomes essentially Lorentzian at temperatures of $180\text{ }^{\circ}\text{C}$ and above, but because we truncate the bands at $\pm 150\text{ cm}^{-1}$ in order to calculate correlation functions, a small value of τ_i is still determined.

There would appear to be a clear relationship between the inhomogeneous broadening of the 1583 cm^{-1} band, the T_g , and the dynamical crossover temperatures T_A and/or T_c (about 448 K or $175\text{ }^{\circ}\text{C}$ for *a*-PS). Because the behavior of the 1583 cm^{-1} band differs significantly to that of the 1601 cm^{-1} mode, we suggest that this sensitivity is a result of the apparent anharmonic coupling of the former to the 1592 cm^{-1} combination mode that becomes evident at elevated temperature. At temperatures up to near the T_g , the 1592 cm^{-1} combination mode is relatively weak but becomes increasingly prominent above temperatures of about $80\text{ }^{\circ}\text{C}$.¹⁸ As a result, below this temperature the modulation that inhomogeneously broadens the 1583 cm^{-1} band is "slow" (in vibrational spectroscopic terms), of the order of 2 ps, and is probably a result of the same factors that affect the 1601 cm^{-1} mode. At temperatures near the T_g , however, coupling to the 1592 cm^{-1} mode increases significantly. This introduces a degree of sensitivity to dynamical transitions, presumably because anharmonic coupling of the modes is mediated by lattice or bath modes.⁶ At high temperatures, above about $170\text{--}180\text{ }^{\circ}\text{C}$, the band shape of the 1583 cm^{-1} mode (essentially Lorentzian) indicates that the modulation is very fast, and the effects of local differences in environment are averaged out by a rapid "loss of memory". Between 80 and $\sim 180\text{ }^{\circ}\text{C}$ (T_A or T_c), there is a crossover regime, where inhomogeneous broadening at first increases, then decreases, and becomes negligible at temperatures greater than $180\text{ }^{\circ}\text{C}$. It appears that the mode of vibrational relaxation is changing as *a*-PS is cooled from high temperatures into this crossover regime and polymer chain segments start to become trapped in a cage of their neighbors.

The contribution of inhomogeneous broadening to the overall second moment of the band is shown in Figure 13. It can be seen that the distribution of local environments that is superimposed upon the distribution sampled by static inhomogeneous broadening (i.e., that which reflects the distribution of environments encountered at very short times, $t \rightarrow 0$) is small.

These observations are consistent with both modified MCT and RFOT theories, which predict that at temperatures above $\sim 1.2T_g$ (about 448 K or $175\text{ }^{\circ}\text{C}$ for *a*-PS) the time scale for molecular collisions and the interchange of positions are about the same. In RFOT theory, at temperature below T_A , molecules or segments keep the same set of neighbors for an extended time (hundreds of collisions). Interconversion between local structures occurs as a result of small local rearrangements, which slow with temperature but persist below the laboratory T_g . Relative to the static distribution of environments that would be characteristic of a frozen instance in time, such local rearrangements would be expected to superimpose only a small increase in inhomogeneous broadening, as observed. Activated hopping processes below T_c would have a similar effect in modified MCT.

The results presented here are also consistent with molecular dynamics simulation studies of *a*-PS by Roe⁴⁸ and Lyulin et al.^{49,50} These authors identified two distinct regimes of translational mobility in molecular dynamics simulation studies. At times shorter than about 1 ps, the motions of the segments are unconstrained by their neighbors, but at times greater than this the constraining effect of neighbors becomes apparent. At temperatures well above the T_g , there is a changeover from short time ballistic to long time diffusive behavior. In the crossover region, segments are temporarily trapped in a cage of their

neighbors until some thermally activated process leads to an escape from the cage. Inhomogeneous broadening of the 1583 cm^{-1} mode appears to be directly related to these dynamics.

Conclusions

Conformationally insensitive bands such as the ring modes of atactic polystyrene can be used to calculate time correlation functions that are influenced by the dynamics of the system, through dephasing processes, vibrational energy relaxation, or (probably) both. These time correlation functions can be modeled in terms of two processes: a fast modulation and a second slower modulation that inhomogeneously broadens the bands. The fast modulation is of the order of 0.014 ps for both modes studied here. Librational motions of the phenyl ring occur on the 0.01 ps time scale, suggesting that this mode of relaxation involves a rapid dephasing process. A slower process that has a relaxation time of the order of a few picoseconds and is relatively insensitive to temperature inhomogeneously broadens a band near 1601 cm^{-1} . This type of behavior mirrors the so-called "fast" transition seen in neutron diffraction studies of this polymer. One cannot draw firm conclusions, however, because dephasing and vibrational energy relaxation mechanisms cannot be separated by studies of simple band shapes alone. However, these results suggest that the application of nonlinear techniques to a study of atactic polystyrene in this frequency range would provide considerable insight into the dynamics of this polymer.

A second fundamental mode, near 1583 cm^{-1} , is also inhomogeneously broadened, but the relaxation time calculated for this mode is far more sensitive to temperature, as a result of anharmonic coupling to a combination mode that is probably mediated by lattice or bath modes. This provides a path for vibrational energy relaxation and sensitivity to dynamical transitions. A change in the modulation of the 1583 cm^{-1} band becomes apparent about $10\text{--}20\text{ }^{\circ}\text{C}$ below the thermally measured T_g . Relaxation times at first increase (from about 2 ps to near 10 ps) and then decrease and become negligible at temperatures near $180\text{ }^{\circ}\text{C}$. These results are consistent with theories of the glass transition, which predict a dynamical transition near $1.2T_g$. As the melt is cooled to this temperature, segments begin to reside within a cage of their neighbors and persistent local structures are formed. Interconversion between these structures continues as the sample is cooled through a crossover region but near the experimentally observed T_g becomes so slow that only a fraction of the rearrangements have time to occur.

Acknowledgment. The authors gratefully acknowledge the support of the National Science Foundation, Polymers Program, under Grant DMR-0551465, and the Korea Research Foundation (KRF-2003-013-D00023).

References and Notes

- (1) Doge, G.; Yarwood, J. *Infrared and Raman Studies on Molecular Dynamics in Liquids*. In *Spectroscopy and Relaxation of Molecular Liquids*; Steele, D., Yarwood, J., Eds.; Elsevier: Amsterdam, 1991; Chapter 6.
- (2) Rothschild, W. D. *Dynamics of Molecular Liquids*; John Wiley & Sons: New York, 1984.
- (3) Oxtoby, D. W. *Adv. Chem. Phys.* **1979**, *40*, 1.
- (4) Kirillov, S. A. *J. Mol. Liq.* **1998**, *76*, 35.
- (5) Rothschild, W. G. *J. Phys. Chem.* **1976**, *65*, 455.
- (6) Rothschild, W. G.; Cavagnat, R. M. *J. Chem. Phys.* **1992**, *97*, 2900.
- (7) Cataliotti, R. S.; Foggi, P.; Giorgini, M. G.; Mariani, L.; Morresi, A.; Paliani, G. *J. Chem. Phys.* **1993**, *98*, 4372.
- (8) Navarro, R.; Bratu, I.; Henanz, A. J. *Phys. Chem.* **1993**, *97*, 9081.
- (9) Yi, J.; Jonas, J. J. *Phys. Chem.* **1996**, *100*, 16789.
- (10) Stolov, A. A.; Herrebout, W. A.; van der Veken, B. J.; Remizov, A. B. *J. Phys. Chem. B* **1998**, *102*, 6493.
- (11) Kirillov, S. A.; Yannopoulos, S. N. *J. Chem. Phys.* **2002**, *117*, 1220.

- (12) Kirillov, S. A.; Voyiatzis, I. S.; Musiyenko, G. M.; Photiadis, G. M.; Pavlatou, E. A. *J. Chem. Phys.* **2001**, *114*, 3683.
- (13) Kalampounias, A. G.; Yannopoulos, S. N.; Steffen, W.; Kirillova, L. I.; Kirillov, S. A. *J. Chem. Phys.* **2003**, *118*, 8340.
- (14) Perrot, M.; Rothschild, W. G.; Cavagnat, R. M. *J. Chem. Phys.* **1999**, *110*, 9230.
- (15) Oxtoby, D. W. *J. Chem. Phys.* **1981**, *74*, 1503.
- (16) Mariani, L.; Moretti, A.; Cataliotti, R. S.; Giorgini, M. G. *J. Chem. Phys.* **1996**, *104*, 914.
- (17) Kirillov, S. A. *Chem. Phys. Lett.* **1999**, *303*, 37.
- (18) Painter, P.; Sobkowiak, M.; Park, Y. *Macromolecules* **2007**, *40*, 1730.
- (19) Painter, P.; Sobkowiak, M.; Park, Y. *Macromolecules* **2007**, *40*, 1738.
- (20) Loring, R. F.; Mukamel, S. *J. Chem. Phys.* **1985**, *83*, 2116–2128.
- (21) Kanaya, T.; Kaji, K. *Adv. Polym. Sci.* **2001**, *154*, 87.
- (22) Zorn, R. *J. Phys.: Condens. Matter* **2003**, *15*, R1025.
- (23) Das, S. P. *Rev. Mod. Phys.* **2004**, *76*, 785.
- (24) Reichman, D. R.; Charbonneau, P. *J. Stat. Mech.* **2005**, P05013.
- (25) Lubchenko, V.; Wolynes, P. G. *Annu. Rev. Phys. Chem.* **2007**, *58*, 235.
- (26) Ngai, K. L. *Comments Solid State Phys.* **1979**, *9*, 121.
- (27) Ngai, K. L. *J. Phys.: Condens. Matter* **2000**, *12*, 6437.
- (28) Ngai, K. L.; Capaccioli, S. *J. Phys.: Condens. Matter* **2007**, *19*, 205114.
- (29) Ngai, K. L. *Philos. Mag.* **2004**, *84*, 1341.
- (30) Das, S. P.; Mazenko, G. F. *Phys. Rev. A* **1986**, *34*, 2265.
- (31) Gotze, W.; Sjogren, L. *J. Phys. C* **1988**, *21*, 3407.
- (32) Bhattacharyya, S. M.; Bagchi, B.; Wolynes, P. W. *Phys. Rev. E* **2005**, *72*, 31509.
- (33) Hall, R. W.; Wolynes, P. G. *J. Phys. Chem. B* **2008**, *112*, 301.
- (34) Xia, X.; Wolynes, P. G. *Proc. Natl. Acad. Sci. U.S.A.* **2000**, *97*, 2990.
- (35) Kitpatrick, T. R.; Wolynes, P. G. *Phys. Rev. E* **1987**, *35*, 3072.
- (36) Painter, P. C.; Koenig, J. L. *J. Polym. Sci., Polym. Phys. Ed.* **1977**, *15*, 1885.
- (37) Snyder, R. G.; Painter, P. C. *Polymer* **1981**, *22*, 1633.
- (38) Liu, Y.; Lin, J.; Huang, G.; Guo, Y.; Duan, C. *J. Opt. Soc. Am. B* **2001**, *18*, 666.
- (39) Enns, J. B.; Boyer, R. F.; Ishida, H.; Koenig, J. L. *Polym. Eng. Sci.* **1979**, *19*, 756.
- (40) Graf, R. T.; Koenig, J. L.; Ishida, H. *Appl. Spectrosc.* **1985**, *39*, 405.
- (41) Kubo, R. In *Fluctuations, Relaxation and Resonance in Magnetic Systems*; ter Haar, G., Ed.; Plenum: New York, 1962.
- (42) George, S. M.; Auweter, H.; Harris, C. B. *J. Chem. Phys.* **1980**, *73*, 5573–5583.
- (43) Oxtoby, D. W. *J. Chem. Phys.* **1981**, *74*, 5371–5376.
- (44) Schweitzer, K. S.; Chandler, D. *J. Chem. Phys.* **1982**, *76*, 2296.
- (45) Schmidt, J. R.; Sundlass, N.; Skinner, J. L. *Chem. Phys. Lett.* **2003**, *378*, 559–566.
- (46) Tiller, A. R. *Macromolecules* **1992**, *25*, 4605.
- (47) Kenkre, V. M.; Tokmakoff, A.; Fayer, M. D. *J. Chem. Phys.* **1994**, *101*, 10618.
- (48) Roe, R. J. *J. Non-Cryst. Solids* **1998**, *235–237*, 308.
- (49) Lyulin, A. V.; Michels, M. A. J. *Macromolecules* **2002**, *35*, 1463.
- (50) Lyulin, A. V.; Balabaev, N. K.; Michels, M. A. J. *Macromolecules* **2002**, *35*, 9595.

MA801900M